ASTRONOMY & ASTROPHYSICS
SUPPLEMENT SERIES

JANVIER **2001**, PAGE 1

Astron. Astrophys. Suppl. Ser. **1**, 1-99 (2001)

The Crab and Galactic Anticentre region observed by COMPTEL

A.W. Strong[1], K. Bennett [4], H. Bloemen [2], H. de Boer [2], R. Buccheri [5], M. Busetta [4], W. Collmar [1], A. Connors [3], R. Diehl [1], J.W. den Herder[2], W. Hermsen [2], L. Kuiper [2], J. Lockwood [3], G.G. Lichti [1], J. Macri [3], M. McConnell [3], D. Morris [3], R. Much [1], J. Ryan [3], V. Schönfelder [1], G. Simpson [3], J.G. Stacy [3], H. Steinle [1], B. Swanenburg [2], M. Varendorff [1], C. Winkler [4] and C. de Vries [2]

[1] Max-Planck Institut für extraterrestrische Physik, D-8046 Garching, FRG,
[2] Laboratory for Space Research, Leiden, P.B. 9504, NL-2300 RA Leiden, The Netherlands
[3] University of New Hampshire, Institute for the Study of Earth, Oceans and Space, Durham NH 03824, USA
[4] Astrophysics Division, Space Science Department of ESA/ESTEC, NL-2200 AG Noordwijk, The Netherlands
[5] IFCAI/CNR, Piazza G. Verdi 6, 90139 Palermo, Italy

Received; accepted

Abstract. — The Galactic anticentre region including the Crab nebula has been observed with the COMPTEL γ - ray telescope on the Gamma Ray Observatory. A map of the region in the 1-30 MeV energy range is presented. The total spectrum of the Crab is derived as well as that of the pulsed and unpulsed components. Upper limits on the pulsar Geminga are also presented.

Key words: gamma rays – pulsars: Crab

1. Introduction

The imaging Compton telescope COMPTEL is one of four instruments on board the Compton Gamma Ray Observatory satellite launched on April 5, 1991. COMPTEL operates in the 0.8 to 30 MeV range with a field of view of 1 steradian, a position location accuracy for bright sources of about 0.5^o and an energy resolution better than 10% FWHM. The instrument is described in Schönfelder et al. (1984); an explanation of the response is given in Diehl et al. (1991).

2. Observations

The Galactic anticentre was observed on three occasions during the first few months of the GRO mission; the observations used here are summarized in Table 1.

TABLE 1. *Summary of COMPTEL observations of the Anticentre region*

Period	l	b	Start	End
Valid.	193.4	-4.3	28 Apr	04 May 91
	184.5	-5.9	04 May	07 May 91
Obs. 1	190.9	-4.7	16 May	30 May 91

Send offprint requests to: A.W.Strong

The 'Validation' observation at the start of the mission was used to verify the correct functioning of the instrument for scientific purposes, the region containing the Crab being chosen since this serves as an excellent 'calibration source'.

3. Maximum entropy maps of the anticentre

The deconvolution of COMPTEL data by the Maximum Entropy Method (MEM) to produce intensity skymaps is described in Strong et al. (1991). The dataspace used had a binning of 1^o in the spatial coordinates and 2^o in the measured Compton scatter angle $\bar{\varphi}$. The background was estimated by averaging over the $\bar{\varphi}$ direction in the 3-D dataspace, and this background is used by the MEM software. As a result of this averaging, smooth extended features are not visible in present MEM image.

Figure 1 shows the image in the 1-30 MeV energy range. Separate images have also been made in the 3 standard sub-ranges 1-3, 3-10 and 10-30 MeV; the Crab source is clearly visible in each case and the position of the maximum has been confirmed to lie in the pixel containing the true position, verifying the directional accuracy of the COMPTEL pointing and the imaging software. No other sources are visible; in particular Geminga (2CG195+4: l=195.1^o,b=$+4.2^o$) is not seen in any of the energy ranges and only an upper limit on the flux (see Sec. 6) can be set.

FIGURE 1 Maximum entropy image of the Galactic anticentre in the 1-30 MeV energy range

4. Total spectrum of the Crab

The total flux from the Crab in the three standard energy ranges was derived by fitting using a maximum-likelihood method. The instrumental response, in particular the point-spread-function (PSF), is energy-dependent so that derivation of a flux over an energy range requires the assumption of an input energy spectrum; in practice the flux is not very sensitive to the assumed spectrum and a single iteration using the spectrum found from the initial assumption is sufficient to obtain a self-consistent result. The uncertainty in the measured fluxes is at present dominated by our knowledge of the instrument response, and is here conservatively taken to be 35% when plotting the spectra. Future refinements of the PSF model should improve the absolute accuracy.

TABLE 2. *Flux measurements of Crab emission as explained in the text. For each energy range the flux is given in units of $10^{-4} cm^{-2} s^{-1}$. For the measured fluxes the fitted number of counts is also given in parentheses.*

	Energy (MeV) 1-3		3-10		10-30	
Total	9.5	(9051)	3.4	(3291)	0.69	(316)
I_1	7.1	(7041)	2.4	(2298)	0.55	(251)
I_2	2.4	(2410)	1.0	(993)	0.15	(65)
I_P	3.4		0.85		0.33	
I_N	6.1		2.5		0.37	

The spectrum is shown in Fig 2 together with results from other experiments. The agreement with HEAO-A4 at low energies and with the extrapolated COS-B results at high energies is excellent. The fluxes in the three ranges are consistent with a power-law; a maximum likelihood fit to a single power law gives $I(E_\gamma) = 1.48 \times 10^{-3} E_{MeV}^{-2.05} cm^{-2} s^{-1} MeV^{-1}$.

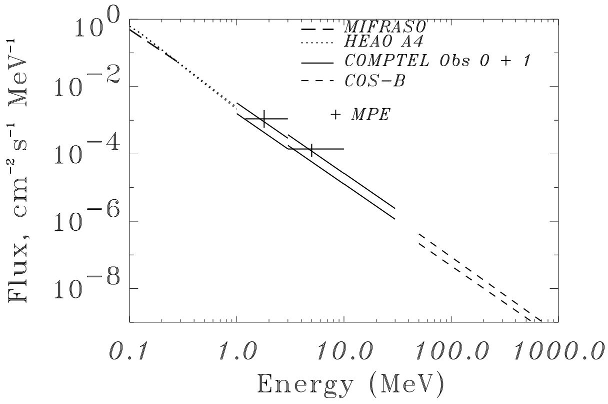

FIGURE 2 Total Spectrum of Crab . Data from MIFRASO: Perotti et al. (1991), HEAO-A4: Jung (1989), MPE : Graser and Schönfelder 1982, COMPTEL: this work, COS-B: Clear et al. (1987)

5. Spectrum of the pulsar and DC component

The COMPTEL results for the Crab pulsar γ - ray lightcurve are presented in Bennett et al. (1992). This shows that the pulsed phase interval containing the two peaks is 0.2-0.8. Denoting the 'pulsed' and 'unpulsed' phase fluxes by I_1 and I_2 respectively and the pulsed phase interval by f (=0.6) we have $I_1 = fI_N + I_P$ and $I_2 = (1-f)I_N$ where I_N and I_P are the DC (usually assumed to come from the nebula) and pulsar fluxes respectively. Hence $I_N = I_2/(1-f)$, $I_P = I_1 - I_2 f/(1-f)$. Fitting the events in the pulsed and unpulsed phase intervals with the instrumental response yields I_1 and I_2; the results are given in Table 2, together with the resulting I_P and I_N.

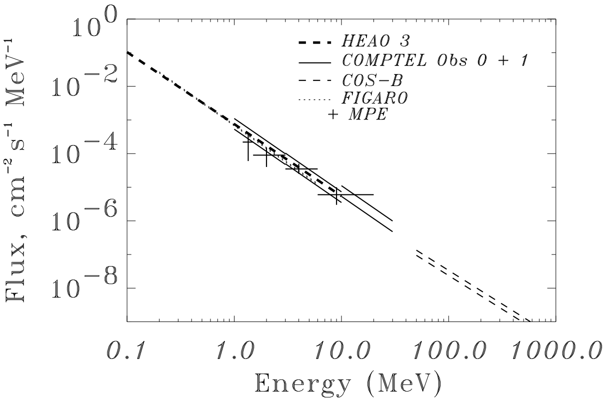

FIGURE 3 Spectrum of Crab pulsar. Data from HEAO 3: Mahoney et al. (1984), MPE: Graser and Schönfelder 1982, COMPTEL: this work, COS-B: Clear et al. (1987)

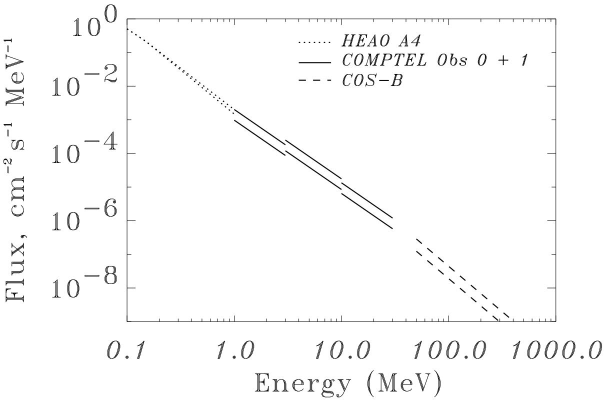

FIGURE 4 Spectrum of Crab DC component. Data from HEAO-A4: Jung (1989), COMPTEL: this work, COS - B: Clear et al. (1987)

From Table 2, the Crab flux is 35% pulsed over the full 1-30 MeV energy range. Figure 3 shows the spectrum of the Crab pulsar. A maximum likelihood fit to a single power law gives I(E_γ)= $5.5\times10^{-4}E_{MeV}^{-2.2}$cm^{-2}s^{-1}MeV^{-1}. The pulsar spectrum is fully consistent with results from other experiments as shown in Figure 3 and with an extrapolation to the COS-B spectrum given in Clear et al. (1987). For the DC component (Figure 4) a maximum likelihood fit to a single power law gives I(E_γ)= $9.4\times10^{-4}E_{MeV}^{-2.0}$cm^{-2}s^{-1}MeV^{-1}; this does not appear to confirm a continuation of the steepening to -2.5 above 150 keV reported by Jung (1989) from HEAO-A4 data. The absolute flux at 1 MeV is however quite consistent with the HEAO-A4 spectrum. The COMPTEL data do not however appear to be completely consistent with a constant power law over the 1-30 MeV range; there is a possible steepening in the 3-10 MeV range which requires further evaluation. An extrapolation to 100 MeV is consistent with the COS-B spectrum reported by Clear et al. (1987).

In the model of De Jager and Harding (1991) the DC component of γ - rays is generated by synchrotron radiation from shock accelerated electrons beyond the pulsar wind shock. Comparing with their model predictions, electrons with energies up to at least $3\times\ 10^{15}$ eV would be required to generate the spectrum observed by COMPTEL.

6. Geminga upper limits

The fits to the anticentre region (Section 4) included a source at the Geminga pulsar (2CG195+4) position, and this yielded an upper limit to the flux in each energy range. Figure 5 shows our (2σ) upper limits together with the spectrum from Grenier et al. (1991) based on a deconvolution of COS-B data and also upper limits from the SIGMA experiment (Lebrun et al. 1991). The COS-B spectrum falls off steeply below 100 MeV and this is consistent with the non-detection by COMPTEL and SIGMA. One COS-B measurement however did show a power-law increase to lower energies; an extrapolation of this spectrum would be marginally inconsistent with the present limits.

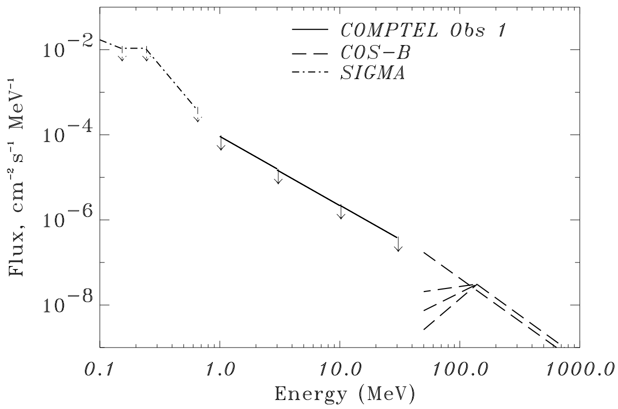

FIGURE 5 Spectrum of Geminga pulsar. Data from SIGMA (Lebrun et al. 1991), COMPTEL: this work, COS-B: Grenier et al. (1991)

Acknowledgements.

I thank F. Lebrun for useful comments on the SIGMA results

.

References

Agrinier B. et al., 1990, Astrophys. J. 355 , 645
Bennett K. et al. 1992, *these proceedings*
Clear J. et al.,1987, Astron. Astrophys. , 174 , 85
De Jager O.C., Harding A.K., 1991, Proc. 22nd Int. Cosmic Ray Conf., 1, 572
Diehl R. et al., 1991, in Data Analysis in Astronomy IV , Plenum, New York
Graser U., Schönfelder V., 1982, Astrophys. J. 263 ,677
Grenier, I.A., Hermsen, W., Hote, C., 1991, Adv. Space Res. Vol 11, No. 8, 107
Jung G.V., 1989, Astrophys. J. , 338 , 972
Lebrun F. et al., 1991, Proc. 22st Int. Cosmic Ray Conf. 1 , 165
Perotti F. et al., 1991, Astrophys. J. , 373 , 75
Schönfelder V. et al., 1984, IEEE Trans. Nucl. Sci., NS-31, 766
Strong A.W. et al., 1990, Proc. 21st Int. Cosmic Ray Conf. 4 , 154
Strong A.W. et al. , 1991, in 'Data Analysis in Astronomy IV' , Plenum, New York